Int. J. Solids Structures Vol. 29, No. 6, pp. 767–781, 1992
Printed in Great Britain.

0020-7683/92 $5.00 + .00

WAVE PROPAGATION IN LAMINATED COMPOSITE CIRCULAR CYLINDERS

N. RATTANAWANGCHAROEN and A. H. SHAH
Department of Civil Engineering, University of Manitoba, Winnipeg, Manitoba, Canada R3T 2N2

and

S. K. DATTA
Department of Mechanical Engineering and CIRES, University of Colorado, Boulder, CO 80309, U.S.A.

(*Received* 18 *June* 1990; *in revised form* 12 *June* 1991)

Abstract—A stiffness method is used to study the dispersion characteristics of waves propagating in laminated composite cylinders. Each lamina of the cylinder can possess distinct anisotropic properties, mass density and thickness. The objective of the study is to analyze the effects of the circumferential wave number, ply lay up configuration, number of layers, and the thickness-to-radius ratio on the dispersion characteristics. A Rayleigh–Ritz type of approximation of the through-thickness variation of the displacements which maintains the continuity of displacements and tractions at the interfaces between the layers has been used. The numerical results are compared with those obtained from the method using quadratic interpolation functions and also with the analytical solutions to illustrate the accuracy and efficiency of the method. Frequency spectra for four ply $[+30\ -30]_s$ and $[+15/-15]_s$, sixteen ply $[+15/-15]_4$, and twelve ply $[0_3/+45/-45/0_3]$, graphite/epoxy laminated composite cylinders are also presented. Numerical results show strong influence of anisotropy on the guided waves.

INTRODUCTION

The role of laminated composite structures composed of fibre-reinforced members for space environments is widely recognized. Fibre-reinforced laminated composite tubes are currently being studied as candidate struts for trusses to be used in space structures. To improve their utilization, their physical behaviour needs to be understood. Therefore, analysis of wave propagation in laminated composite cylinders is becoming of interest among many researchers. A comprehensive knowledge of wave scattering plays an important role in identifying cracks in cylinders. One approach to solving the wave scattering problem is to represent the scattered field by wave function expansion, as reported for plates by Abduljabbar *et al.* (1983). In order to represent the scattered wave field by the wave function expansion, displacement and stress eigenfunctions have to be accurately established.

The vibrations of an infinitely long, circular cylinder are governed by the dispersion equation. This equation, which relates the frequency and the wavelength, requires the field equations of linear elasticity to be satisfied throughout the cylinder and the lateral surfaces of the cylinder to be free of traction. Wave propagation in homogeneous isotropic cylinders has been thoroughly studied analytically (Pochhammer, 1876; Onoe *et al.*, 1962; Gazis, 1959; Armenàkas *et al.*, 1969). A considerable amount of information exists concerning the vibration and wave propagation in isotropic composite circular cylinders. McNiven *et al.* (1963) studied the propagation of axisymmeric longitudinal harmonic waves in a solid rod encased by an outer rod of finite thickness. Armenàkas (1965, 1967, 1971) studied the propagation of torsional harmonic waves in composite rods and also derived the frequency equation for the propagation of harmonic waves in a two-layered shell with arbitrary circumferential modes, and presented the frequency spectrum of two-layered isotropic shells. Jai-Lue Lai (1971) studied the propagation of the harmonic waves in the elastic solid rod with elastic rod casing and presented the model for soft core with stiff casing. Not many analytical works for anisotropic cylinders have been reported. Axisymmetric waves in homogeneous orthothopic cylinders were considered by Mirsky (1964) and McNiven and Mengi (1971), while asymmetric problems were solved by Chou and Achenbach (1972) and

Armenàkas and Reitz (1973) using Frobenius series. To our knowledge, no exact solutions for laminated anisotropic cylinders are available.

Since the mathematical manipulation involved in deriving the frequency equations for anisotropic cylinders is cumbersome and their solution intractable, many researchers have studied the vibration in laminated orthotropic cylinders by approximate theories. The most common ones are shell theories. A list of references on various approximate cylindrical shell theories can be found in the recent papers by Khdeir *et al.* (1989) and Barbero and Reddy (1990). However, shell theories are cumbersome to use and they do not provide accurate eigenvalues required for wave scattering problems. Theories which yield accurate eigenvalues and are computationally very convenient to use are theories derived through the stiffness method of analysis. Nelson *et al.* (1971) and Huang and Dong (1984) presented a stiffness method to study wave propagation in laminated anisotropic cylinders with an arbitrary number of lamina. They discretized the cylinder in the thickness direction into mathematical sublayers and used interpolation functions that involved only the displacements at the interfaces between sublayers and at the middle of the sublayers as the generalized coordinates. Although the technique generally yields good results for the frequency spectrum, it does not directly lead to the evaluation of the tractions at the interface boundaries. In order to use a hybrid model to study the scattering from cracks and inhomogeneities (Abduljabbar *et al.*, 1983; Koshiba *et al.*, 1984), it is necessary to get accurate results for both displacements and tractions. With this application in mind, we present in this paper a stiffness method which incorporates the displacements and tractions at the interfaces between sublayers as generalized coordinates. A similar technique was used by Datta *et al.* (1989) to study dispersion of waves in a laminated plate.

In the stiffness method used in this study, the dynamic behaviour of a composite cylinder is approximated by dividing the cylinder into several sublayers and representing the displacement distribution through the thickness of each sublayer by polynomial interpolation functions. These functions are chosen to satisfy the displacement and stress continuity at the interfaces between the adjoining sublayers. By applying Hamilton's principle, the dispersion equation is obtained as a standard algebraic eigenvalue problem. Eigenvalues and eigenvectors of this equation yield the frequencies and the associated displacements and tractions of propagating and evanescent modes.

The accuracy of the stiffness method is demonstrated by comparing the results with the analytical solutions and the results obtained by the method employed by Huang and Dong for homogeneous isotropic cylinders. Effects of circumferential wave number, ply lay up configuration, thickness-to-radius ratio and the number of layers on the dispersion characteristics in fibre-reinforced angle-ply cylinders are investigated.

FORMULATION

Time harmonic elastic wave propagation in an infinite circular cylinder composed of perfectly bonded lamina with possibly distinct mechanical properties, as shown in Fig. 1, is considered here. Two lateral surfaces of the cylinder, i.e. the inner and the outer surfaces, are free of traction. The direction of wave propagation is z.

Governing equations

In this method, each lamina is divided into several sublayers so that the total number of sublayers through the thickness H is N. It is assumed that the kth sublayer of thickness h_k with inner and outer radii r_k and r_{k+1} can possess distinct anisotropic moduli C_{pq} ($p, q = 1, 2, \ldots, 6$) and density ρ_k. With reference to the cylindrical coordinates (r, θ, z), the stress–strain relation in the kth sublayer is given by:

$$\{\sigma\} = [C]\{\varepsilon\}, \tag{1}$$

where

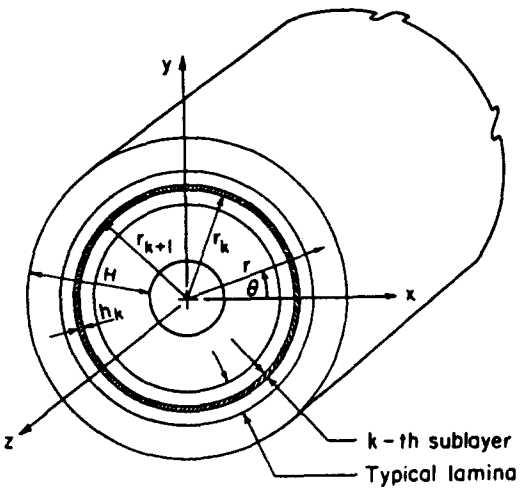

Fig. 1. Geometry of laminated cylinder.

$$\{\sigma\}^T = \langle \sigma_{rr} \quad \sigma_{\theta\theta} \quad \sigma_{zz} \quad \tau_{\theta z} \quad \tau_{rz} \quad \tau_{r\theta} \rangle,$$
$$\{\varepsilon\}^T = \langle \varepsilon_{rr} \quad \varepsilon_{\theta\theta} \quad \varepsilon_{zz} \quad \gamma_{\theta z} \quad \gamma_{rz} \quad \gamma_{r\theta} \rangle.$$

Let the radial, circumferential and axial displacements (u, v, w) be assumed in the forms:

$$u(r, \theta, z; t) = \tilde{u}(r, z; t)\, e^{im\theta},$$
$$v(r, \theta, z; t) = \tilde{v}(r, z; t)\, e^{im\theta},$$
$$w(r, \theta, z; t) = \tilde{w}(r, z; t)\, e^{im\theta}, \tag{2}$$

where t denotes time, m the circumferential wave number and $i = \sqrt{-1}$. The strain - displacement relationship can then be written as:

$$\varepsilon_{rr} = \frac{\partial \tilde{u}}{\partial r} e^{im\theta},$$
$$\varepsilon_{\theta\theta} = \left(\frac{\tilde{u}}{r} + im\frac{\tilde{v}}{r}\right) e^{im\theta},$$
$$\varepsilon_{zz} = \frac{\partial \tilde{w}}{\partial z} e^{im\theta},$$
$$\gamma_{\theta z} = \left(\frac{\partial \tilde{v}}{\partial z} + im\frac{\tilde{w}}{r}\right) e^{im\theta},$$
$$\gamma_{rz} = \left(\frac{\partial \tilde{u}}{\partial z} + \frac{\partial \tilde{w}}{\partial r}\right) e^{im\theta},$$
$$\gamma_{r\theta} = \left(im\frac{\tilde{u}}{r} + \frac{\partial \tilde{v}}{\partial r} - \frac{\tilde{v}}{r}\right) e^{im\theta}. \tag{3}$$

The factor $e^{im\theta}$ will be suppressed in the sequel.

Stiffness method

The displacements at a point in the kth sublayer approximated by interpolation polynomials in the radial direction can be written as:

$$\{U\} = [N_1]\{q'\} + [N_2]\{q\}, \tag{4}$$

where

$$\{U\}^{\mathrm{T}} = \langle \tilde{u} \quad \tilde{v} \quad \tilde{w} \rangle,$$

$$\{q\}^{\mathrm{T}} = \langle \tilde{u}_k \quad \tilde{\sigma}_k \quad \tilde{v}_k \quad \tilde{\tau}_k \quad \tilde{w}_k \quad \tilde{\chi}_k \quad \tilde{u}_{k+1} \quad \tilde{\sigma}_{k+1} \quad \tilde{v}_{k+1} \quad \tilde{\tau}_{k+1} \quad \tilde{w}_{k+1} \quad \tilde{\chi}_{k+1} \rangle.$$

$[N_1]$ and $[N_2]$ are given in Appendix A. Prime in eqn (4) denotes differentiation with respect to z. The generalized coordinates $\tilde{u}_k$, $\tilde{v}_k$, $\tilde{w}_k$, $\tilde{\sigma}_k$, $\tilde{\tau}_k$ and $\tilde{\chi}_k$ are the values of $\tilde{u}$, $\tilde{v}$, $\tilde{w}$, $\tilde{\sigma}_{rr}$, $\tilde{\tau}_{rz}$ and $\tilde{\tau}_{r\theta}$, respectively, at the kth interface. Subscript $k+1$ denotes the same quantities at the $(k+1)$th interface. These nodal values of the displacement and traction components are functions of z and t.

The equations governing the nodal generalized coordinates $\tilde{u}_k$, $\tilde{v}_k$, $\tilde{w}_k$, $\tilde{\sigma}_k$, $\tilde{\tau}_k$ and $\tilde{\chi}_k$ $(k = 1, \ldots, N+1)$ are obtained using Hamilton's principle. The Lagrangian, L_k for the kth sublayer is calculated as:

$$L_k = \frac{1}{2}\int_t \int_z \left\{ \int_{r_k}^{r_{k+1}} (\rho_k \{\dot{\bar{U}}\}^{\mathrm{T}} \{\dot{U}\} - \{\bar{\varepsilon}\}^{\mathrm{T}} [C] \{\varepsilon\}) r \, \mathrm{d}r \right\} \mathrm{d}z \, \mathrm{d}t. \tag{5}$$

In eqn (5), overbar and overdot denote complex conjugate and time differentiation respectively. Using eqn (4) in strain–displacement relations (3), these in turn in (5), and summing the contributions from all sublayers and upon setting its first variation to zero leads to the following equation (Datta *et al.*, 1989):

$$[K_1]\{Q''\} + [K_2]\{Q'''\} + \{[E_1]\{Q''\} - [C_1]\{\ddot{Q}''\}\} + \{[E_2]\{Q'\} - [C_2]\{\ddot{Q}'\}\} + \{[E_3]\{Q\} + [M]\{\ddot{Q}\}\} = 0. \tag{6}$$

The generalized displacement traction vector $\{Q\}$ and the matrices $[C_1]$, $[C_2]$, $[M]$, $[K_1]$, $[K_2]$ and $[E_1]$ through $[E_3]$ are defined in Appendix A. Note that the matrices $[C_1]$ and $[K_1]$ are real and symmetric, $[M]$, $[E_1]$ and $[E_3]$ are Hermitian, while $[C_2]$, $[K_2]$ and $[E_2]$ are skew-Hermitian.

Algebraic eigenvalue problems

A solution for eqn (6) can be assumed in the form:

$$\{Q(z;t)\} = \{Q_0\} \, \mathrm{e}^{\mathrm{i}\omega t} \mathrm{e}^{-\gamma z} \tag{7}$$

where $\{Q_0\}$ represents the nodal amplitude vector, ω the circular frequency and γ the complex wave number. Substitution of eqn (7) into eqn (6) results in a set of linear homogeneous equations as:

$$[\gamma^4[K_1] - \gamma^3[K_2] + \gamma^2[K_3] - \gamma[K_4] + [K_5]]\{Q_0\} = 0, \tag{8}$$

where

$$\begin{aligned} [K_3] &= [E_1] + \omega^2[C_1], \\ [K_4] &= [E_2] + \omega^2[C_2], \\ [K_5] &= [E_3] - \omega^2[M]. \end{aligned} \tag{9}$$

For a non-trivial solution, the determinant of the coefficient matrix must be zero which results in the eigenvalue problem denoted as EVP-I. This equation is the dispersion relation to solve for the eigenvalue γ for given ω. Alternatively, when γ is specified, the generalized eigenvalue problem denoted as EVP-II is obtained from eqn (8) as:

$$[K_\gamma]\{Q_0\} = \omega^2[M_\gamma]\{Q_0\} \tag{10a}$$

where

$$[K_\gamma] = \gamma^4[K_1] - \gamma^3[K_2] + \gamma^2[E_2] - \gamma[E_1] + [E_3],$$
$$[M_\gamma] = [M] + \gamma[C_1] - \gamma^2[C_2]. \tag{10b}$$

The complex wave number, γ, is admissible only in the form of:

$$\gamma = \gamma_R - i\gamma_I \tag{11}$$

where

$$\gamma_R \geqslant 0.$$

The propagation mode occurs when $\gamma_R = 0$. In contrast, if $\gamma_I = 0$ and $\gamma_R \neq 0$ the mode is evanescent or non-propagating. When γ_R and γ_I are both non-zero, edge vibration in which motion is confined near the edge is possible. It can be seen from eqn (8) that if γ is an eigenvalue, then $-\bar{\gamma}$ is also an eigenvalue.

NUMERICAL RESULTS AND DISCUSSION

The method outlined above was implemented in a computer code to determine the eigenvalues and eigenvectors of the EVP-I and EVP-II (eqns (8) and (10)). For brevity, frequency spectra for only propagating modes (EVP-II) are presented. The frequency spectra in all examples are plotted for the normalized frequency Ω and the normalized wave number ξ. In all examples considered below H and R are the total thickness and mean radius of the cylinders, respectively. To demonstrate the accuracy, effectiveness and versatility of the proposed method, numerical results for the following six examples are presented:

(1) Homogeneous isotropic cylinder with the Poisson's ratio, ν, of 0.3, $H/R = 1.5$ and circumferential wave numbers, m, of 1 and 3.
(2) A 4-ply $[+30/-30]$, graphite/epoxy cylinder, $H/R = 0.667$ and circumferential wave numbers, m, of 1 and 3.
(3) A 4-ply $[+15/-15]$, graphite/epoxy cylinder, $H/R = 0.667$ and circumferential wave numbers, m, of 1 and 3.
(4) A 4-ply $[+15/-15]$, graphite/epoxy cylinder, $H/R = 0.10$, and a circumferential wave number, m, of 1 and 3.
(5) A 16-ply $[+15/-15]$, graphite/epoxy cylinder, $H/R = 0.10$ and a circumferential wave number, m, of 1.
(6) A 12-ply $[0_2/+45/-45/0_2]$, graphite/epoxy cylinder, $H/R = 0.10$ and a circumferential wave number, m, of 1.

The finite element models consist of eight sublayers for the first four examples, 16 sublayers for the fifth example, and 12 sublayers for the last example. There are no perceptible changes in the frequency spectra observed in every example by increasing the number of sublayers. In all figures, the analytical solutions are represented by the circle, the method used by Huang and Dong by the dotted line and the present method by the solid line.

In the first example, the normalized frequency and the normalized wave number are given by:

$$\Omega = \frac{\omega H}{\pi c_s}, \quad \xi = \frac{\gamma H}{\pi}$$

where

$$v_s = \left[\frac{\mu}{\rho}\right]^{1/2},$$

and μ is the shear modulus. Figures 2a and 2b show the frequency spectra for this example. Comparing the results from the Huang and Dong method, the present method and the analytical solution which contains the Bessel functions (Armenàkas *et al.*, 1969), it can be observed that the present method yields results that are in excellent agreement with the analytical solution. For higher modes and or larger wave numbers, the discrepancy between the two approximate methods becomes noticeable. The circumferential wave number does not affect the pattern of the discrepancy of the results.

For the rest of the examples, the elastic properties for each ply relative to their natural elastic axes are (Huang and Dong, 1984):

$$E_L = 13.9274 \times 10^{10}\ \text{N m}^{-2}, \quad E_T = 1.5169 \times 10^{10}\ \text{N m}^{-2};$$
$$G_{LT} = G_{TT} = 0.5861 \times 10^{10}\ \text{N m}^{-2}, \quad \nu_{LT} = \nu_{TT} = 0.21.$$

The normalized frequency and the normalized wave number are given by:

$$\Omega = \frac{\omega H}{v_L}, \quad \xi = \frac{\gamma H}{\pi}$$

where

$$v_L = \left[\frac{E_L}{\rho}\right]^{1/2}.$$

It can be seen from Figs 3a and 3b, for example 2, that the circumferential wave number does not affect the pattern of the discrepancy between the two approximate methods. However, the change in circumferential wave number from 1 to 3 is quite pronounced in alteration of the dispersion characteristics. The rigid body motion does not appear when the circumferential wave number is 3.

To illustrate the effect of ply lay up configuration, the frequency spectra for example 3 are shown in Figs 4a and 4b. The circumferential wave number shows a similar effect as in the case of $[+30/-30]$, ply lay up tube of example 2. Comparing Figs 3a and 3b with Figs 4a and 4b for the same circumferential wave number, it can be observed that the orientation of the fibres leads to the change in the dispersion characteristics. It can be seen from Figs 3b and 4b that when $m = 3$, there are more backward waves; a phenomenon associated with the region of the frequency spectrum having group and phase velocity of opposite signs (Meeker and Meitzler, 1964), for $[+30/-30]$, ply lay up.

The frequency spectra of the tubes with $H/R = 0.10$, corresponding to relatively thin tubes, are presented in Figs 5–7 for examples 4–6, respectively. Figures 4 and 5 illustrate the influence of the H/R ratio on the dispersion characteristics. When the circumferential wave number is 1, the change in the H/R ratio does not significantly alter the frequency spectra. All the effects, however, are localized in the region having both low wave numbers and low frequencies. The influence of the H/R ratio becomes more pronounced for the circumferential wave number of 3. It can be noticed from Figs 5a and 5b that, for relatively thin tubes, the change in circumferential wave number from 1 to 3 does not lead to the change of dispersion characteristics. Figures 5a and 6 show that the effect of layering (i.e. the number of layers) is significant. Layering has a tendency to increase phase velocities. Figure 7 shows the frequency spectra for example 6 which is a multi-angle symmetric lamina used in the aerospace industry. It can be noticed, from Fig. 7, that the phase velocities approach the constant phase velocity stage more slowly than in the cases of $[+15/-15]$, or $[+30/-30]$, ply lay up tubes.

From Figs 2–7, it can be seen that the results obtained by the present method are always lower than those obtained by the Huang and Dong method. Both the stiffness

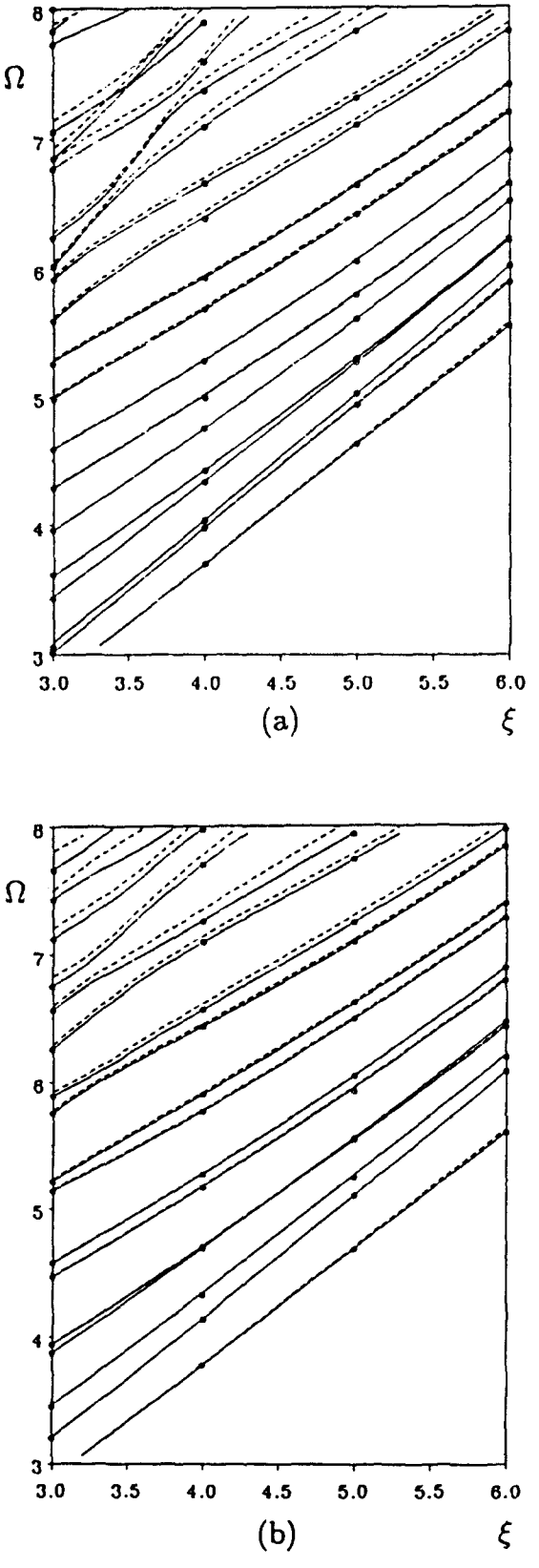

Fig. 2. Frequency spectra for a homogeneous isotropic cylinder with $\nu = 0.3$, $H/R = 1.5$ (a) $m = 1$; (b) $m = 3$.

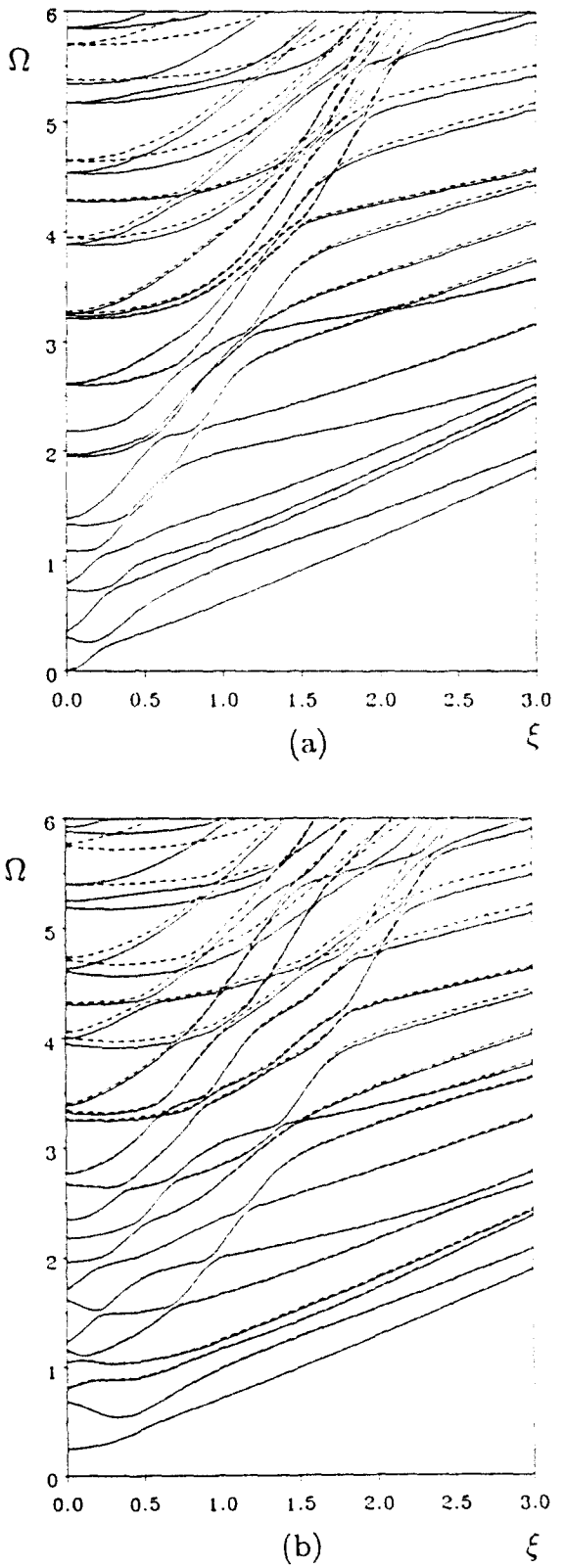

Fig. 3. Frequency spectra for a 4-ply [+30° −30], graphite/epoxy cylinder with $H/R = 0.667$ (a) $m = 1$; (b) $m = 3$.

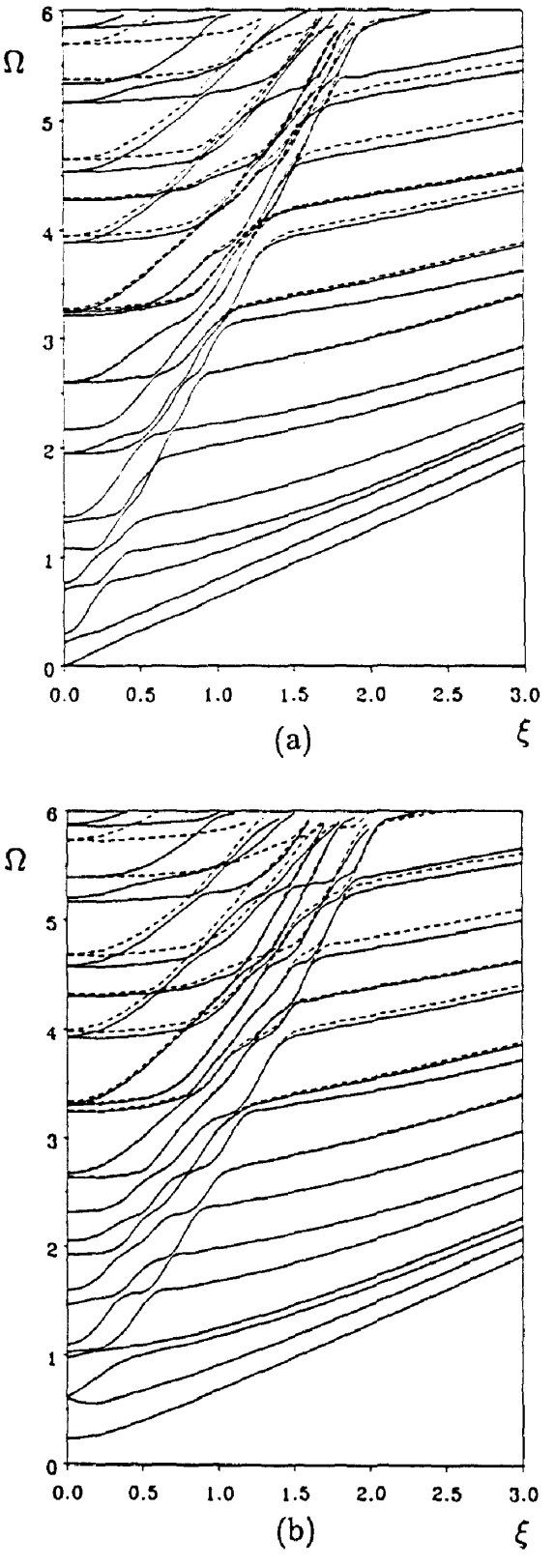

Fig. 4. Frequency spectra for a 4-ply [+15/−15], graphite/epoxy cylinder with $H/R = 0.667$ (a) $m = 1$; (b) $m = 3$.

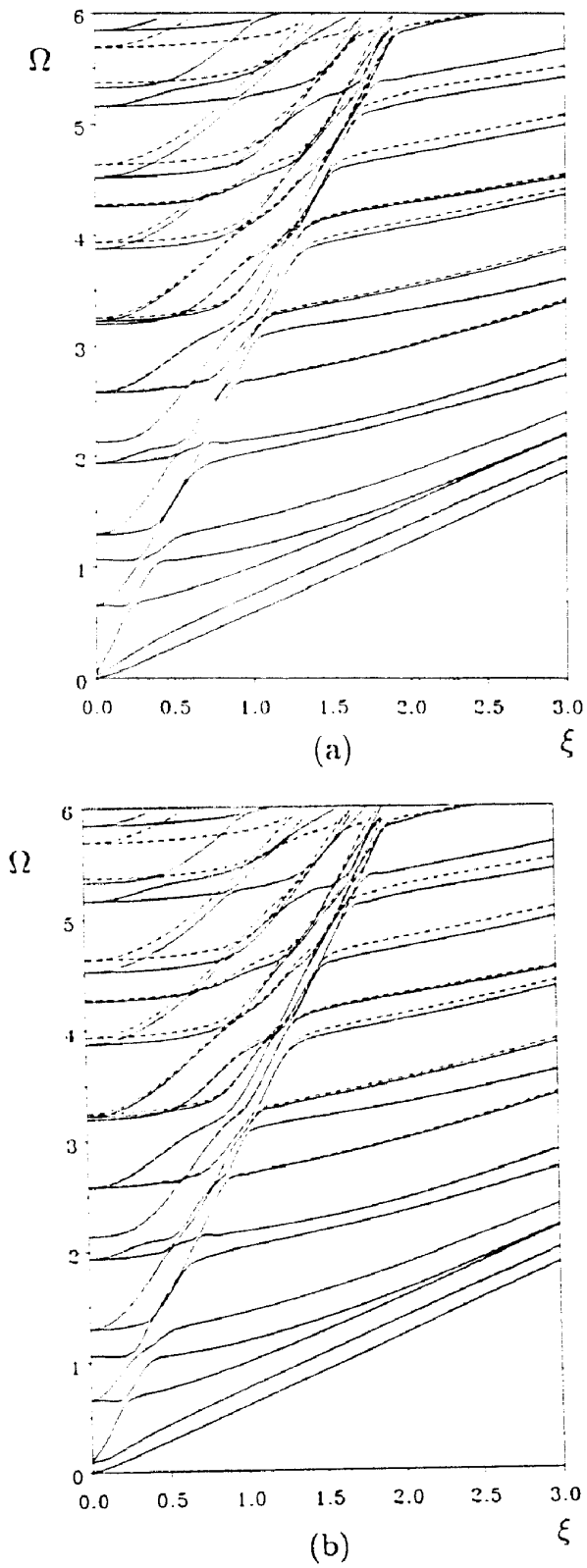

Fig. 5. Frequency spectra for a 4-ply [+15 −15], graphite epoxy cylinder with $H/R = 0.10$ (a) $m = 1$; (b) $m = 3$.

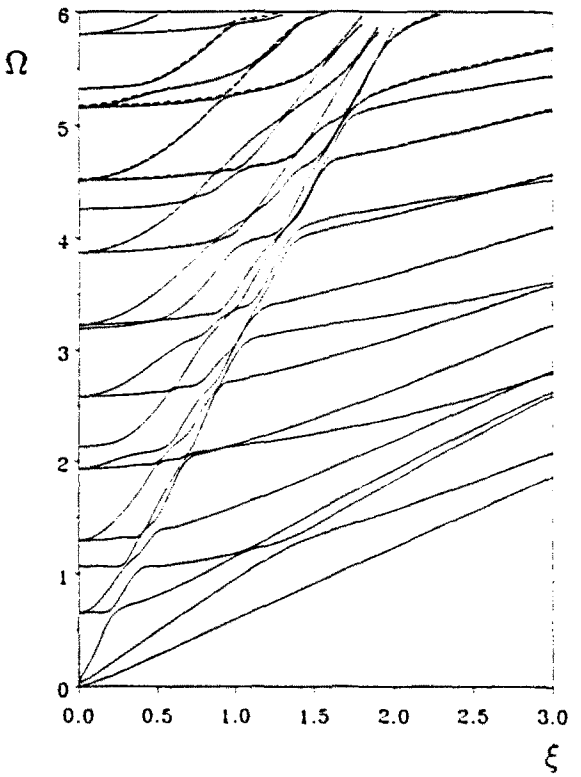

Fig. 6. Frequency spectra for a 16-ply $[+15/-15]_4$ graphite/epoxy cylinder with $H/R = 0.10$ and $m = 1$.

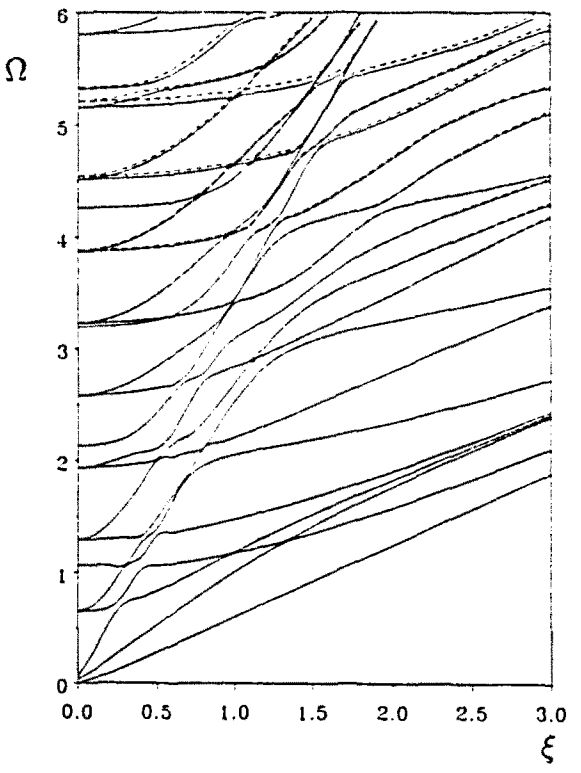

Fig. 7. Frequency spectra for a 12-ply $[0_2/+45/-0_2]_s$ graphite/epoxy cylinder with $H/R = 0.10$ and $m = 1$.

methods use the consistent mass approach. Thus, it can be concluded that the present method yields results closer to the analytical results.

CONCLUSION

A stiffness method based on through-thickness cubic interpolation functions for the displacements that maintain continuity of displacement and traction components at the interfaces between the sublayers has been used to study guided wave propagation in laminated composite cylinders. This method yields more accurate results than those obtained from the stiffness method employing quadratic interpolations which ensures the continuity of only the displacement components. It may be noted that for the same number of sublayers modelled in EVP-II, the present method provides the smaller number of degrees of freedom which, consequently, reduces the computational time. The numerical results presented show that dispersion characteristics significantly depend upon fibre orientation and number of layers, and to a lesser degree on thickness-to-radius ratio. The effect of the circumferential wave number on dispersion characteristics is significant only for the thick cylinders in the low frequencies and low wave numbers regime.

Acknowledgements—The work presented in this paper was supported by the Natural Science and Engineering Research Council of Canada grant OGP007988. Partial support was also received from the office of Naval Research grant N00014-86-K-0280 (Program officer: Dr. Y. Rajapakse). The authors appreciate the information and helpful suggestions given by Mr. S. Rajpal, Boeing Canada Technology Ltd., Winnipeg.

REFERENCES

Abduljabbar, Z., Datta, S. K. and Shah, A. H. (1983). Diffraction of horizontally polarized shear waves by normal edge cracks in a plate. *J. Appl. Phys.* **52**, 461–472.

Armenàkas, A. E. (1965). Torsional waves in composite rods. *J. Acoust. Soc. Am.* **38**, 439–446.

Armenàkas, A. E. (1967). Propagation of harmonic waves in composite circular cylindrical shells, Part I—Theoretical investigation. *AIAA Jl* **5**, 740–744.

Armenàkas, A. E. (1971). Propagation of harmonic waves in composite circular cylindrical shells, Part II—Numerical analysis. *AIAA Jl* **9**, 599–605.

Armenàkas, A. E., Gazis, D. C. and Herrmann, G. (1969). *Free Vibrations of Circular Cylindrical Shells*. Pergamon Press, Oxford.

Armenàkas, A. E. and Reitz, E. S. (1973). Propagation of harmonic waves in orthotropic circular cylindrical shells. *J. Appl. Mech.* **40**, 168–174.

Barbero, E. J. and Reddy, J. N. (1990). General two-dimensional theory of laminated cylindrical shells. *AIAA Jl* **28**(3), 544–553.

Chou, F. H. and Achenbach, J. D. (1972). Three dimensional vibration of orthotropic cylinders. *J. Engng Mech. Div. ASCE*. pp. 813–822.

Datta, S. K., Shah, A. H., Brattan, R. L. and Chakraborty, T. (1989). Wave propagation in laminated composite plates. *J. Acoust. Soc. Am.* **83**(6), 2020–2026.

Gazis, D. C. (1959). Three-dimensional investigation of the propagation of waves in hollow circular cylinders—I. Analytical foundation II. Numerical results. *J. Acoust. Soc. Am.* **31**, 568–578.

Huang, K. H. and Dong, S. B. (1984). Propagation waves and edge vibrations in anisotropic composite cylinders. *J. Sound and Vib.* **96**, 363–379.

Jai-Lue Lai (1971). Propagation of harmonic waves in composite elastic cylinder. *J. Acoust. Soc. Am.* **49**, 220–228.

Khdeir, A. A., Reddy, J. N. and Frederick, D. (1989). A study of bending, vibration and buckling of cross-ply circular cylindrical shells with various shell theories. *Int. J. Engng Sci.* **27**(11), 1337–1351.

Koshiba, M., Karakida, S. and Suzuki, M. (1984). Finite-element analysis of Lamb wave scattering in an elastic plate waveguide. *IEEE Trans. Sonics Ultrason.* SU-31, 18.

McNiven, H. D. and Mengi, Y. (1971). Dispersion of waves in transversely isotropic rods. *J. Acoust. Soc. Am.* **49**, 229–236.

McNiven, H. D. Sackman, J. L. and Shah, A. H. (1963). Dispersion of axially symmetric waves in composite, elastic rods. *J. Acoust. Soc. Am.* **35**, 1602–1609.

Meeker, T. R. and Meitzler, A. H. (1964). Guided wave propagation in elongated cylinders and plates. In *Physical Acoustics: Principles and Methods* (Edited by W. P. Mason), pp. 116–167. Academic Press, New York.

Mirsky, I. (1964). Axisymmetric vibrations of orthotropic cylinders. *J. Acoust. Soc. Am.* **36**, 2106–2122.

Nelson, R. B., Dong, S. B. and Kalra, R. D. (1971). Vibration and waves in laminated orthotropic circular cylinders. *J. Sound and Vib.* **18**, 429–444.

Onoe, M., McNiven, H. D. and Mindlin, R. D. (1962). Dispersion of axially symmetric waves in elastic rods. *J. Appl. Mech.* **29**, 729–734.

Pochhammer, L. (1876). Ueber die fortpflanzungsgeshwindigkeiten schwingungen in einem unbegrenzten isotropen kreiscylinder. *Zeitschrift fur Mathematik* **81**, 324–336.

APPENDIX A

The non-zero elements of 3×12 matrices $[N_1]$ and $[N_2]$ of eqn (4) are as follows:

$$N_1(1,3) = \frac{f_2 P_3}{\Delta}, \qquad N_1(3,1) = -f_2,$$
$$N_1(1,5) = \frac{f_2 P_2}{\Delta}, \qquad N_1(3,3) = \frac{f_2 P_9}{\Delta},$$
$$N_1(2,3) = \frac{f_2 P_6}{\Delta}, \qquad N_1(3,5) = \frac{f_2 P_8}{\Delta},$$
$$N_1(2,5) = \frac{f_2 P_5}{\Delta}. \tag{A1}$$

$$N_2(1,1) = f_1 + \frac{f_2 P_1}{\Delta r_k}, \qquad N_2(2,4) = \frac{f_2 \Delta_{33}}{\Delta},$$
$$N_2(1,2) = \frac{f_2 \Delta_{11}}{\Delta}, \qquad N_2(2,5) = \text{im}\,\frac{f_2 P_6}{\Delta r_k},$$
$$N_2(1,3) = \text{im}\,\frac{f_2 P_1}{\Delta r_{k+1}}, \qquad N_2(2,6) = \frac{f_2 \Delta_{23}}{\Delta},$$
$$N_2(1,4) = \frac{f_2 \Delta_{13}}{\Delta}, \qquad N_2(3,1) = \frac{f_2 P_7}{\Delta r_k},$$
$$N_2(1,5) = \text{im}\,\frac{f_2 P_3}{\Delta r_k}, \qquad N_2(3,2) = \frac{f_2 \Delta_{12}}{\Delta},$$
$$N_2(1,6) = \frac{f_2 \Delta_{12}}{\Delta}, \qquad N_2(3,3) = \text{im}\,\frac{f_2 P_7}{\Delta r_k},$$
$$N_2(2,1) = \frac{f_2 P_4}{\Delta r_k} - \text{im}\,\frac{f_2}{r_k}, \qquad N_2(3,4) = \frac{f_2 \Delta_{23}}{\Delta},$$
$$N_2(2,2) = \frac{f_2 \Delta_{11}}{\Delta}, \qquad N_2(3,5) = f_1 + \text{im}\,\frac{f_2 P_9}{\Delta r_k},$$
$$N_2(2,3) = f_1 + \frac{f_2}{r_k} + \text{im}\,\frac{f_2 P_4}{\Delta r_k}, \qquad N_2(3,6) = \frac{f_2 \Delta_{22}}{\Delta}. \tag{A2}$$

The parameters P_l are given by:

For $l = 1, 2, 3$; $j = l+1$:

$$P_l = -\begin{vmatrix} C_{1j} & C_{15} & C_{16} \\ C_{5j} & C_{55} & C_{56} \\ C_{6j} & C_{65} & C_{66} \end{vmatrix}.$$

For $l = 4, 5, 6$; $j = l-2$:

$$P_l = \begin{vmatrix} C_{11} & C_{1j} & C_{14} \\ C_{51} & C_{5j} & C_{55} \\ C_{61} & C_{6j} & C_{65} \end{vmatrix}. \tag{A3}$$

For $l = 7, \ldots, 10$; $j = l-5$:

$$P_l = -\begin{vmatrix} C_{11} & C_{1j} & C_{16} \\ C_{51} & C_{5j} & C_{56} \\ C_{61} & C_{6j} & C_{66} \end{vmatrix},$$
$$\Delta = P_{10}.$$

Δpq is the cofactor of element C_{pq} of matrix Δ. Functions f_n $(n = 1, 2, 3, 4)$ are cubic polynomials given by:

$$f_1 = \tfrac{1}{4}(2 - 3\eta + \eta^3), \qquad f_2 = \tfrac{1}{4}(2 + 3\eta - \eta^3),$$
$$f_3 = \frac{h_k}{8}(1 - \eta - \eta^2 + \eta^3), \quad f_4 = \frac{h_k}{8}(-1 - \eta + \eta^2 + \eta^3), \tag{A4}$$

where

$$\eta = \frac{1}{h_k}(2r - r_{k+1} - r_k),$$
$$h_k = r_{k+1} - r_k.$$

The matrices $[C_1]$, $[C_2]$, $[M]$, $[K_1]$, $[K_2]$ and $[E_1]$ through $[E_3]$ in eqn (6) are given by:

$$[C_1] = \int_0^H \rho[N_1]^T[N_1] r \, dr,$$
$$[C_2] = \int_0^H \rho\left[[N_1]^T[N_2] - [\bar{N}_2]^T[N_1]\right] r \, dr,$$
$$[M] = \int_0^H \rho[\bar{N}_2]^T[N_2] r \, dr,$$
$$[K_1] = \int_0^H [d]^T[C][d] r \, dr,$$
$$[K_2] = \int_0^H [d]^T[C][b] r \, dr,$$
$$[E_1] = \int_0^H \left[[d]^T[C][a] - [\bar{b}]^T[C][b] + [\bar{a}]^T[C][d]\right] r \, dr,$$
$$[E_2] = \int_0^H \left[[\bar{a}]^T[C][b] - [\bar{b}]^T[C][a]\right] r \, dr,$$
$$[E_3] = \int_0^H [\bar{a}]^T[C][a] r \, dr. \tag{A5}$$

where overbar indicates complex conjugate.

The non-zero elements of 6×12 matrix $[a]$ in eqn (A5) are as follows:

$$a(1,1) = f_{1,r} + \frac{f_{2,r}P_1}{\Delta r_k},$$
$$a(1,2) = \frac{f_{2,r}\Delta_{11}}{\Delta},$$
$$a(1,3) = \text{im}\,\frac{f_{2,r}P_1}{\Delta r_k},$$
$$a(1,4) = \frac{f_{2,r}\Delta_{11}}{\Delta},$$
$$a(1,5) = \text{im}\,\frac{f_{2,r}P_1}{\Delta r_k},$$
$$a(1,6) = \frac{f_{2,r}\Delta_{12}}{\Delta},$$
$$a(2,1) = \frac{f_1}{r} + \frac{m^2 f_2}{r_k r} + \frac{f_2 P_1}{\Delta r_k r} + \text{im}\,\frac{f_2 P_4}{\Delta r_k r},$$
$$a(2,2) = \frac{f_2\Delta_{11}}{\Delta r} + \text{im}\,\frac{f_2\Delta_{13}}{\Delta r},$$
$$a(2,3) = -\frac{m^2 f_2 P_4}{\Delta r_k r} + \frac{\text{im}}{r}\left(f_1 + \frac{f_2}{r_k} + \frac{f_2 P_1}{\Delta r_k}\right),$$
$$a(2,4) = \frac{f_2\Delta_{13}}{\Delta r} + \text{im}\,\frac{f_2\Delta_{11}}{\Delta r},$$
$$a(2,5) = -\frac{m^2 f_2 P_6}{\Delta r_k r} + \text{im}\,\frac{f_2 P_3}{\Delta r_k r},$$
$$a(2,6) = \frac{f_2\Delta_{12}}{\Delta r} + \text{im}\,\frac{f_2\Delta_{21}}{\Delta r},$$
$$a(4,1) = \text{im}\,\frac{f_2 P_7}{\Delta r_k r},$$
$$a(4,2) = \text{im}\,\frac{f_2\Delta_{12}}{\Delta r},$$
$$a(4,3) = -\frac{m^2 f_2 P_7}{\Delta r_k r},$$
$$a(4,4) = \text{im}\,\frac{f_2\Delta_{21}}{\Delta r},$$
$$a(4,5) = -\frac{m^2 f_2 P_9}{\Delta r_k r} + \text{im}\,\frac{f_1}{r},$$
$$a(4,6) = \text{im}\,\frac{f_2\Delta_{22}}{\Delta r},$$
$$a(5,1) = \frac{f_{2,r}P_7}{\Delta r_k},$$
$$a(5,2) = \frac{f_{2,r}\Delta_{12}}{\Delta},$$
$$a(5,3) = \text{im}\,\frac{f_{2,r}P_7}{\Delta r_k},$$
$$a(5,4) = \frac{f_{2,r}\Delta_{21}}{\Delta},$$
$$a(5,5) = f_{1,r} + \text{im}\,\frac{f_{2,r}P_9}{\Delta r_k},$$
$$a(5,6) = \frac{f_{2,r}\Delta_{22}}{\Delta},$$
$$a(6,1) = \frac{P_4}{\Delta r_k}\left(f_{2,r} - \frac{f_2}{r}\right) + \text{im}\left(\frac{f_1}{r} + \frac{f_2 P_1}{\Delta r_k r} + \frac{f_2}{r_k r} - \frac{f_{2,r}}{r_k}\right),$$
$$a(6,2) = \frac{\Delta_{13}}{\Delta}\left(f_{2,r} - \frac{f_2}{r}\right) + \text{im}\,\frac{f_2\Delta_{11}}{\Delta r},$$

$$a(6,3) = f_{1,r} + \frac{f_{2,r}}{r_k} - \frac{f_1}{r} - \frac{f_2}{r_k r} - \frac{m^2 f_2 P_1}{\Delta r_k r} + \text{im}\frac{P_4}{\Delta r_k r}\left(f_{2,r} - \frac{f_2}{r}\right),$$

$$a(6,4) = \frac{\Delta_{33}}{\Delta}\left(f_{2,r} - \frac{f_2}{r}\right) + \text{im}\frac{f_2\Delta_{13}}{\Delta r},$$

$$a(6,5) = -\frac{m^2 f_2 P_3}{\Delta r_k r} + \text{im}\frac{P_6}{\Delta r_k}\left(f_{2,r} - \frac{f_2}{r}\right),$$

$$a(6,6) = \frac{\Delta_{23}}{\Delta}\left(f_{2,r} - \frac{f_2}{r}\right) + \text{im}\frac{f_2\Delta_{12}}{\Delta r}, \tag{A6}$$

where the $f_{n,r}$ represents $\partial f_n/\partial r$.

The non-zero elements of 6×12 matrix $[b]$ in eqn (A5) are as follows:

$$b(1,3) = \frac{f_{2,r}P_3}{\Delta}, \qquad b(4,3) = f_1 + \frac{f_2}{r_k} + \text{im}\frac{f_2}{\Delta}\left(\frac{P_4}{r_k} + \frac{P_9}{r}\right),$$

$$b(1,5) = \frac{f_{2,r}P_2}{\Delta}, \qquad b(4,4) = \frac{f_2\Delta_{33}}{\Delta},$$

$$b(2,3) = \frac{f_2P_3}{\Delta r} + \text{im}\frac{f_2P_6}{\Delta r}, \qquad b(4,5) = \text{im}\frac{f_2}{\Delta}\left(\frac{P_6}{r_k} + \frac{P_8}{r}\right),$$

$$b(2,5) = \frac{f_2P_2}{\Delta r} + \text{im}\frac{f_2P_5}{\Delta r}, \qquad b(4,6) = \frac{f_2\Delta_{23}}{\Delta},$$

$$b(3,1) = \frac{f_2P_7}{\Delta r_k}, \qquad b(5,1) = f_1 + f_{2,r} + \frac{f_2P_1}{\Delta r_k},$$

$$b(3,2) = \frac{f_2\Delta_{12}}{\Delta}, \qquad b(5,2) = \frac{f_2\Delta_{11}}{\Delta},$$

$$b(3,3) = \text{im}\frac{f_2P_7}{\Delta r_k}, \qquad b(5,3) = \frac{f_{2,r}P_9}{\Delta} + \text{im}\frac{f_2P_1}{\Delta r_k},$$

$$b(3,4) = \frac{f_2\Delta_{23}}{\Delta}, \qquad b(5,4) = \frac{f_2\Delta_{13}}{\Delta},$$

$$b(3,5) = f_1 + \text{im}\frac{f_2P_9}{\Delta r_k}, \qquad b(5,5) = \frac{f_{2,r}P_8}{\Delta} + \text{im}\frac{f_2P_3}{\Delta r_k},$$

$$b(3,6) = \frac{f_2\Delta_{22}}{\Delta}, \qquad b(5,6) = \frac{f_2\Delta_{12}}{\Delta},$$

$$b(4,1) = \frac{f_2P_4}{\Delta r_k} - \text{im}f_2\left(\frac{l}{r_k} + \frac{l}{r}\right), \qquad b(6,3) = \frac{P_6}{\Delta}\left(f_{2,r} - \frac{f_2}{r}\right) + \text{im}\frac{f_2P_3}{\Delta r},$$

$$b(4,2) = \frac{f_2\Delta_{13}}{\Delta}, \qquad b(6,5) = \frac{P_5}{\Delta}\left(f_{2,r} - \frac{f_2}{r}\right) + \text{im}\frac{f_2P_2}{\Delta r}. \tag{A7}$$

The 6×12 matrix $[d]$ in eqn (A5) has non-zero elements as follows:

$$d(3,1) = -f_2, \qquad d(4,3) = \frac{f_2P_6}{\Delta},$$

$$d(3,3) = \frac{f_2P_9}{\Delta}, \qquad d(4,5) = \frac{f_2P_5}{\Delta},$$

$$d(3,5) = \frac{f_2P_8}{\Delta}, \qquad d(5,3) = \frac{f_2P_3}{\Delta},$$

$$d(5,5) = \frac{f_2P_2}{\Delta}, \tag{A8}$$

where the remaining six columns of matrices $[N_1]$, $[N_2]$, $[a]$, $[b]$ and $[d]$ can be obtained from the first six columns by replacing f_1 by f_3, f_2 by f_4, and r_k by r_{k+1}.